

Unveiling the composition of the single-charm molecular pentaquarks: insights from M1 radiative decays and magnetic moments

Fu-Lai Wang^{1,2,3,5*} and Xiang Liu^{1,2,3,4,5†}

¹*School of Physical Science and Technology, Lanzhou University, Lanzhou 730000, China*

²*Lanzhou Center for Theoretical Physics, Key Laboratory of Theoretical Physics of Gansu Province, Lanzhou University, Lanzhou 730000, China*

³*Key Laboratory of Quantum Theory and Applications of MoE, Lanzhou University, Lanzhou 730000, China*

⁴*MoE Frontiers Science Center for Rare Isotopes, Lanzhou University, Lanzhou 730000, China*

⁵*Research Center for Hadron and CSR Physics, Lanzhou University and Institute of Modern Physics of CAS, Lanzhou 730000, China*

In order to unravel the composition of the isoscalar DN , D^*N , D_1N , and D_2^*N molecular pentaquarks, this study systematically investigates their electromagnetic properties, including the M1 radiative decays and the magnetic moment properties. Using the constituent quark model and taking into account both the S - D wave mixing effect and the coupled channel effect, our analysis yields numerical results indicating that the M1 radiative decays and the magnetic moment properties of these molecular pentaquarks provide some insights into their inner structures. These results can serve as crucial clues for distinguishing their spin-parity quantum numbers and configurations in experimental studies. In addition, we highlight the importance of the electromagnetic properties as key observables for elucidating the inner structures of the observed $\Lambda_c^+(2940)$ and $\Lambda_c^+(2910)$. We expect that these discoveries will inspire our experimental colleagues to further explore the family of the single-charm molecular pentaquarks and to investigate the inner structures of the $\Lambda_c^+(2940)$ and $\Lambda_c^+(2910)$ in future studies.

I. INTRODUCTION

In the past decades, how to understand the non-perturbative behavior of the strong interaction has received the significant attention from the whole community, especially with more and more observations of new hadronic states reported in different experiments [1–11]. An important reason is that the study of the hadron spectroscopy is one of the most effective approaches to deepen our understanding of the non-perturbative behavior of the strong interaction. Although the hadron family has become more and more abundant with the joint efforts of theorists and experimentalists, the search for exotic states is still an ongoing research issue around the hadron spectroscopy.

Indeed, the observations of more and more new hadronic states close to the corresponding hadronic thresholds have stimulated extensive discussions on the existence of the hadronic molecular states in the past two decades [1–11]. Among them, the explorations of the hidden-charm molecular pentaquarks have achieved the significant breakthroughs [12–22]. As the important experimental progress on the study of the hidden-charm molecular pentaquarks, the LHCb Collaboration observed three resonance structures, namely the $P_\psi^N(4312)$, $P_\psi^N(4440)$, and $P_\psi^N(4457)$ states, when analyzing the $J/\psi p$ invariant mass spectrum in 2019 [13]. This experimental observation provides the direct evidence to support the existence of the $\Sigma_c \bar{D}^{(*)}$ -type hidden-charm molecular pentaquark states in the hadron spectroscopy [16–22]. Given the current research status of the hidden-charm molecular pentaquarks, it is reasonable to speculate about the existence of the single-charm molecular pentaquark candidates in the

hadron spectroscopy.

In 2006, the $\Lambda_c^+(2940)$ was first observed in the $D^0 p$ invariant mass distributions by the BaBar Collaboration [23]. It was later confirmed in the $\Sigma_c(2455)\pi$ decay channel by the Belle Collaboration [24] and the $D^0 p$ channel by the LHCb Collaboration [25]. The most likely spin-parity quantum number assignment for the $\Lambda_c^+(2940)$ is $J^P = 3/2^-$, but the other spin-parity quantum numbers cannot be excluded, as indicated by LHCb [25]. Since there is the low mass puzzle for the observed $\Lambda_c^+(2940)$, the $\Lambda_c^+(2940)$ can be explained as the D^*N molecular state [26–47]. In 2022, the Belle Collaboration reported the discovery of the $\Lambda_c^+(2910)$ by the analysis of the $\Sigma_c(2455)\pi$ invariant mass spectrum [48]. The $\Lambda_c^+(2910)$ was also explained as a D^*N molecular state [47].

We should point out that this is a way to solve the low mass puzzle of the $\Lambda_c^+(2940)$. In fact, recognizing the importance of the unquenched effect, it is still possible to categorize the $\Lambda_c^+(2940)$ as the $2P$ state of singly charmed baryon [49–67]. Obviously, there exist different explanations for the $\Lambda_c^+(2940)$. The situation can happen for the $\Lambda_c^+(2910)$. How to distinguish these different assignments to the $\Lambda_c^+(2940)$ and $\Lambda_c^+(2910)$ is an interesting research topic.

As the important physical observables revealing the inner structure of the hadron, in this work we propose to systematically study the electromagnetic properties including the M1 radiative decay widths and the magnetic moment properties of the isoscalar DN , D^*N , D_1N , and D_2^*N molecular pentaquarks, which will be a main task of the present study. Meanwhile, we also discuss the M1 radiative decay widths and the magnetic moment properties of the observed $\Lambda_c^+(2940)$ and $\Lambda_c^+(2910)$ in the $2P$ states of singly charmed baryon [49–67]. To achieve our goal, we adopt the constituent quark model, which has been widely used in the discussions of the M1 radiative decay widths and the magnetic moment properties of the hadrons in the past decades [68–119]. In our realistic calculations, both the S - D wave mix-

*Electronic address: wangfl2016@lzu.edu.cn

†Electronic address: xiangliu@lzu.edu.cn

ing effect and the coupled channel effect are taken into account, which is similar to the study of their mass spectrum in Refs. [28, 120]. The current investigation can provide some insights into the properties of the single-charm molecular pentaquark candidates and the inner structures of the observed $\Lambda_c^+(2940)$ and $\Lambda_c^+(2910)$, which may inspire our experimental colleagues to further explore the family of the single-charm molecular pentaquarks and to investigate the inner structures of the $\Lambda_c^+(2940)$ and $\Lambda_c^+(2910)$ in future studies.

The present paper is organized as the follows. After Introduction, we primarily study the transition magnetic moments and the corresponding M1 radiative decay widths of the isoscalar DN , D^*N , D_1N , and D_2^*N molecular pentaquarks in Section II. After that, we further discuss the magnetic moment properties of the isoscalar DN , D^*N , D_1N , and D_2^*N molecular pentaquarks in Section III. Among them, we also discuss the M1 radiative decay widths and the magnetic moment properties of the observed $\Lambda_c^+(2940)$ and $\Lambda_c^+(2910)$ in the $2P$ states of singly charmed baryon. Finally, the discussion and conclusion will be provided in Section IV.

II. THE M1 RADIATIVE DECAYS

Before discussing the electromagnetic properties of the single-charm molecular pentaquarks, let's briefly review the research status of their mass spectrum based on the one-boson-exchange model and the chiral effective field theory. In Refs. [26, 28], the authors discussed the D^*N molecular pentaquark candidates using the one-boson-exchange model, and found that several isoscalar D^*N states can be considered as the single-charm molecular pentaquark candidates. In Ref. [42], the authors investigated the DN and D^*N interactions within the chiral effective field theory, and concluded that the isoscalar DN state with $J^P = 1/2^-$ and the isoscalar D^*N states with $J^P = (1/2^-, 3/2^-)$ can be regarded as the single-charm molecular pentaquark candidates. Except for the $D^{(*)}N$ -type single-charm molecular pentaquark candidates, the mass spectrum of the D_1N/D_2^*N -type single-charm molecular pentaquark candidates has also been predicted through the one-boson-exchange model in Ref. [120]. They found that it is easier to form the isoscalar D_1N and D_2^*N molecular states compared to the isovector D_1N and D_2^*N systems [120]. Thus, in the present work we further study the electromagnetic properties including the M1 radiative decay widths and the magnetic moment properties of the isoscalar DN , D^*N , D_1N , and D_2^*N molecular pentaquarks based on the corresponding mass spectrum [26, 28, 42, 120], which can

provide the crucial information for enhancing our knowledge of their spectroscopic behavior.

In comparison to other electromagnetic properties of the hadrons, the radiative decays of the hadronic states may be easier to observe in experimental studies. In particular, the study of the radiative decays of the hadrons can offer the vital insights into their inner structures. As emphasised in Refs. [126–129], the investigation of the radiative decay ratio $R = \mathcal{B}(X(3872) \rightarrow \psi(2S)\gamma)/\mathcal{B}(X(3872) \rightarrow J/\psi\gamma)$ can provide the important information for unveiling the inner structure of the observed $X(3872)$. Thus, the study of the radiative decays of the isoscalar DN , D^*N , D_1N , and D_2^*N molecular pentaquarks can serve as the crucial clues in the experimental construction of the family of the single-charm molecular pentaquark states. In this section, we primarily study the M1 radiative decay widths of the isoscalar DN , D^*N , D_1N , and D_2^*N molecular pentaquarks.

A. The constituent quark model approach

In the past theoretical studies, the radiative decay behavior of the hadrons has been extensively discussed based on various theoretical models and approaches, including the constituent quark model, the chiral perturbation theory, the QCD sum rules, the Bag model, the lattice QCD simulations, and so on [9]. In the present work, we quantitatively study the M1 radiative decay widths of the isoscalar DN , D^*N , D_1N , and D_2^*N molecular pentaquarks by adopting the constituent quark model, which has been widely used in the discussions of the M1 radiative decay widths of the heavy-flavor molecular pentaquarks in recent years [98, 102, 103, 110, 111, 114, 116]. In this subsection, we present how to study the M1 radiative decay widths of the isoscalar DN , D^*N , D_1N , and D_2^*N molecular pentaquarks within the constituent quark model.

According to Refs. [79, 86, 88, 92, 94–100, 102, 103, 107–112, 115, 116, 119, 130], the M1 radiative decay width between the hadronic states $\Gamma_{H \rightarrow H'\gamma}$ can be linked to the corresponding transition magnetic moment $\mu_{H \rightarrow H'}$. Thus, we need to define the transition magnetic moment before discussing the M1 radiative decay width between the hadronic states. In the present work, the influence of the spatial wave functions of the initial and final states is considered when studying the transition magnetic moments and the M1 radiative decay widths between the isoscalar DN , D^*N , D_1N , and D_2^*N molecular pentaquarks. Obviously, the spatial wave functions of the isoscalar DN , D^*N , D_1N , and D_2^*N molecular pentaquarks depend on their binding properties [102, 103, 110, 111, 115, 116, 119]. However, the experimental information on the isoscalar DN , D^*N , D_1N and D_2^*N molecular pentaquarks is currently unavailable [121]. For simplicity, we assume that the binding energies of the initial and final molecular pentaquarks are identical when calculating the transition magnetic moments between the isoscalar DN , D^*N , D_1N , and D_2^*N molecular pentaquarks in the present work. Based on the above assumption, we can deduce the transition magnetic moments between the isoscalar DN , D^*N , D_1N , and D_2^*N molecular pentaquarks by the following rela-

¹ In the present work, D_1 and D_2^* represent the $D_1(2420)$ and $D_2^*(2460)$ mesons [121], respectively. Among them, the $D_1(2420)$ should be considered as the mixture of the 1^1P_1 and 1^3P_1 states, i.e., [122–125]

$$|D_1(2420)\rangle = -\sin\theta_{1P} |1^1P_1\rangle + \cos\theta_{1P} |1^3P_1\rangle. \quad (2.1)$$

In the heavy quark limit, the mixing angle $\theta_{1P} = -54.7^\circ$ can be determined by coupling the orbital angular momentum with the spin angular momentum [122–125].

tion [110, 111, 115, 116, 119]

$$\mu_{H \rightarrow H'} = \left\langle J_{H'}, J_z \left| \sum_j \hat{\mu}_{zj}^{\text{spin}} e^{-i\mathbf{k} \cdot \mathbf{r}_j} + \hat{\mu}_z^{\text{orbital}} \right| J_H, J_z \right\rangle, \quad (2.2)$$

where J_z is the smallest value between the total angular momentum quantum numbers J_H and $J_{H'}$, $e^{-i\mathbf{k} \cdot \mathbf{r}_j}$ is the spatial wave function of the emitted photon for the $H \rightarrow H' \gamma$ process, and \mathbf{k} is the momentum of the emitted photon with $k = (m_H^2 - m_{H'}^2)/2m_H$. In addition, $\hat{\mu}_{zj}^{\text{spin}}$ and $\hat{\mu}_z^{\text{orbital}}$ are the spin magnetic moment operator and the orbital magnetic moment operator, respectively. Their general expressions can be written as [68–113, 115, 116, 119]

$$\hat{\mu}_{zj}^{\text{spin}} = \frac{e_j}{2m_j} \hat{\sigma}_{zj}, \quad (2.3)$$

$$\hat{\mu}_z^{\text{orbital}} = \left(\frac{m_m}{m_b + m_m} \frac{e_b}{2m_b} + \frac{m_b}{m_b + m_m} \frac{e_m}{2m_m} \right) \hat{L}_z, \quad (2.4)$$

respectively. Here, the charge, the mass, and the z -component of the Pauli spin operator of the j -th constituent of the hadronic state are defined as e_j , m_j , and $\hat{\sigma}_{zj}$, respectively. For the orbital magnetic moment operator, the nucleus and the charmed mesons can be differentiated by the subscripts b and m , while we define the z -component of the orbital angular momentum operator between the nucleus and the charmed mesons as \hat{L}_z with $\hat{L}_z Y_{lm} = m Y_{lm}$.

Based on the definition of the transition magnetic moment between the hadronic states $\mu_{H \rightarrow H'}$, we can further give the general expression of the corresponding M1 radiative decay width $\Gamma_{H \rightarrow H' \gamma}$, i.e., [102, 103, 110, 111, 115, 116, 119]

$$\Gamma_{H \rightarrow H' \gamma} = \frac{\alpha_{\text{EM}}}{2J_H + 1} \frac{k^3}{m_p^2} \frac{\sum_{J_{H'z}, J_{Hz}} \begin{pmatrix} J_{H'} & 1 & J_H \\ -J_{H'z} & 0 & J_{Hz} \end{pmatrix}^2}{\begin{pmatrix} J_{H'} & 1 & J_H \\ -J_z & 0 & J_z \end{pmatrix}^2} \frac{|\mu_{H \rightarrow H'}|^2}{\mu_N^2}. \quad (2.5)$$

In the above expression, α_{EM} is the electromagnetic fine structure constant with $\alpha_{\text{EM}} \approx 1/137$, m_p is the mass of the proton, μ_N is the nuclear magneton with $\mu_N = e/2m_p$, and the 3- j coefficient is defined by the notation $\begin{pmatrix} a & b & c \\ d & e & f \end{pmatrix}$.

As mentioned earlier, the spatial wave functions of the isoscalar DN , D^*N , D_1N , and D_2^*N molecular pentaquarks and the corresponding constituent hadrons are the important inputs when studying their transition magnetic moments and M1 radiative decay widths. In the following, we discuss the spatial wave functions of the isoscalar DN , D^*N , D_1N , and D_2^*N molecular pentaquarks and the corresponding constituent hadrons.

- For the isoscalar DN , D^*N , D_1N , and D_2^*N molecular pentaquarks, we adopt the precise spatial wave functions, which can be extracted by solving the coupled channel Schrödinger equation based on the one-boson-exchange effective potentials. For the isoscalar DN and

D^*N molecular states, we can obtain their spatial wave functions according to the one-boson-exchange effective potentials of the $D^{(*)}N$ systems listed in Ref. [131]. For the isoscalar D_1N and D_2^*N molecular states, their spatial wave functions can be obtained based on the numerical results of the case II in Ref. [120], which is due to the sign of $g_{\pi NN}k$ is negative according to the quark model [132].

- For the nucleus and the charmed mesons, the simple harmonic oscillator wave function is used to describe their spatial wave functions in this work [102, 103, 110, 111, 115, 116, 119], where the simple harmonic oscillator wave function is

$$\begin{aligned} \phi_{n,l,m}(\beta, \mathbf{r}) &= \sqrt{\frac{2n!}{\Gamma(n+l+\frac{3}{2})}} L_n^{l+\frac{1}{2}}(\beta^2 r^2) \beta^{l+\frac{3}{2}} e^{-\frac{\beta^2 r^2}{2}} r^l Y_{lm}(\Omega_{\mathbf{r}}). \end{aligned} \quad (2.6)$$

Here, the radial, the orbital, and the magnetic quantum numbers of the hadronic states are defined as n , l , and m , respectively. $L_n^{l+\frac{1}{2}}(x)$ is the associated Laguerre polynomial, and $Y_{lm}(\Omega_{\mathbf{r}})$ is the spherical harmonic function. In our realistic calculations, we need a series of oscillating parameters β in the simple harmonic oscillator wave function, and the values of $\beta_D = 0.601$ GeV, $\beta_{D^*} = 0.516$ GeV, $\beta_{c\bar{q}[1^1 P_1]} = 0.475$ GeV, $\beta_{c\bar{q}[1^3 P_1]} = 0.482$ GeV, and $\beta_{c\bar{q}[1^3 P_2]} = 0.437$ GeV are employed in the present work [133].

Based on the obtained spatial wave functions of the isoscalar DN , D^*N , D_1N , and D_2^*N molecular pentaquarks and the corresponding constituent hadrons, we can consider the influence of the spatial wave functions of the emitted photon, the initial hadron, and the final hadron when studying the transition magnetic moments and the M1 radiative decay widths between the isoscalar DN , D^*N , D_1N , and D_2^*N molecular pentaquarks. In our realistic calculations, the spatial wave function of the emitted photon $e^{-i\mathbf{k} \cdot \mathbf{r}_j}$ must be expressed as the following way [134]

$$e^{-i\mathbf{k} \cdot \mathbf{r}_j} = \sum_{l=0}^{\infty} \sum_{m=-l}^l 4\pi(-i)^l j_l(kr_j) Y_{lm}^*(\Omega_{\mathbf{k}}) Y_{lm}(\Omega_{\mathbf{r}_j}), \quad (2.7)$$

where $j_l(x)$ is the spherical Bessel function, and $Y_{lm}(\Omega_{\mathbf{x}})$ is the spherical harmonic function.

In the above discussions, we have presented how to calculate the transition magnetic moments and the M1 radiative decay widths of the isoscalar DN , D^*N , D_1N , and D_2^*N molecular pentaquarks within the constituent quark model. Besides, we can calculate the magnetic moments of the isoscalar DN , D^*N , D_1N , and D_2^*N molecular pentaquarks by the following relation [68–113, 115, 116, 119]

$$\mu_H = \left\langle J_H, J_H \left| \sum_j \hat{\mu}_{zj}^{\text{spin}} + \hat{\mu}_z^{\text{orbital}} \right| J_H, J_H \right\rangle \quad (2.8)$$

when adopting the constituent quark model.

B. The M1 radiative decays between the isoscalar DN and D^*N molecular pentaquarks

In this subsection, we study the M1 radiative decay widths between the isoscalar DN and D^*N molecular pentaquarks by conducting the single channel analysis, the S - D wave mixing analysis, and the coupled channel analysis, respectively. The flavor wave functions of the isoscalar DN and D^*N systems can be given by coupling the flavor wave functions of the corresponding constituent hadrons, which can be expressed as $|D^{(*)}N\rangle = (|D^{(*)0}p\rangle + |D^{(*)+}n\rangle)/\sqrt{2}$ [26, 28]. Similar to the construction of the flavor wave functions of the isoscalar DN and D^*N systems, their spin wave functions $|S, S_3\rangle$ can be obtained by incorporating the spins of the constituent hadrons. For example, the spin wave function $|S, S_3\rangle$ of the DN state with $J^P = 1/2^-$ can be constructed as follows

$$\left|\frac{1}{2}, \frac{1}{2}\right\rangle_{DN} = |0, 0\rangle_D \otimes \left|\frac{1}{2}, \frac{1}{2}\right\rangle_N, \quad (2.9)$$

where the notations S and S_3 in the spin wave function represent the spin and the spin's third component quantum numbers of the hadronic state, respectively.

Within the constituent quark model, the transition magnetic moments of the hadronic molecular states are the linear combination of the transition magnetic moments or the magnetic moments of the corresponding constituent hadrons [102, 103, 110, 111, 115, 116, 119]. For example, the expressions for the transition magnetic moments of the $D^*N[3/2^-] \rightarrow DN[1/2^-]\gamma$ and $D^*N[1/2^-] \rightarrow D^*N[3/2^-]\gamma$ processes are

$$\mu_{D^*N[3/2^-] \rightarrow DN[1/2^-]} = \frac{1}{6}\mu_{D^{*0} \rightarrow D^0} + \frac{1}{6}\mu_{D^{*+} \rightarrow D^+}, \quad (2.10)$$

$$\mu_{D^*N[1/2^-] \rightarrow D^*N[3/2^-]} = \frac{\sqrt{2}}{6}(\mu_{D^{*0}} + \mu_{D^{*+}}) - \frac{\sqrt{2}}{3}(\mu_p - \mu_n), \quad (2.11)$$

respectively. In addition, the transition magnetic moments and the magnetic moments of the nucleus and the charmed mesons are the linear combination of the magnetic magneton of the corresponding constituent quarks $\mu_q = e_q/2m_q$. For instance, the expressions for the transition magnetic moment of the $D^{*0} \rightarrow D^0\gamma$ process and the magnetic moment of the proton are

$$\mu_{D^{*0} \rightarrow D^0} = \mu_c - \mu_{\bar{u}}, \quad \mu_p = \frac{4}{3}\mu_u - \frac{1}{3}\mu_d, \quad (2.12)$$

respectively. Thus, the effective masses of the quarks are the crucial input parameters when describing the M1 radiative decay widths of the isoscalar DN , D^*N , D_1N , and D_2^*N molecular pentaquarks quantitatively. In the present work, we employ the effective masses of the quarks as $m_u = 0.336$ GeV, $m_d = 0.336$ GeV, and $m_c = 1.680$ GeV to give the numerical results [75], which was extensively applied to study the M1 radiative decay widths and the magnetic moment properties of the hadronic states in the past decades [98, 102, 103, 110, 111, 116, 119]. In the present work, we take the masses of the nucleus and the charmed mesons from the Particle Data Group [121].

First, we adopt the constituent quark model and the effective masses of the quarks mentioned above to calculate the transition magnetic moments and the magnetic moments of the nucleus and the charmed mesons. We then compare our obtained results with other findings to assess the reliability of the above input effective masses of the quarks. In Table I, we present our obtained transition magnetic moments and magnetic moments of the nucleus and the charmed mesons, and compare them with other results [94, 103, 115, 119]. By comparison, we find that our obtained transition magnetic moments and magnetic moments of the nucleus and the charmed mesons are consistent with other results [94, 103, 115, 119]. In particular, our obtained magnetic moments of the proton and the neutron are extremely close to the corresponding experimental values [121]. Thus, our adopted effective masses of the quarks are reasonable when discussing the transition magnetic moments and the magnetic moments of the nucleus and the charmed mesons, and we can provide the reliable theoretical suggestions for the M1 radiative decays of the isoscalar DN , D^*N , D_1N , and D_2^*N molecular pentaquarks in the future experimental studies.

TABLE I: The transition magnetic moments and the magnetic moments of the constituent hadrons of the single-charm molecular pentaquarks, and compared them with other results. Here, the transition magnetic moments and the magnetic moments of the hadrons are in units of μ_N .

	Decays	Our result	Other results
$\mu_{H \rightarrow H'}$	$D^{*0} \rightarrow D^0\gamma$	2.174	2.173 [119], 2.134 [115]
	$D^{*+} \rightarrow D^+\gamma$	-0.539	-0.538 [119], -0.540 [94]
	$D_2^{*0} \rightarrow D_1^0\gamma$	1.275	1.277 [119]
	$D_2^{*+} \rightarrow D_1^+\gamma$	-0.451	-0.452 [119]
μ_H	Hadrons	Our result	Other results
	p	2.793	2.793 [121]
	n	-1.862	-1.913 [121]
	D^{*0}	-1.489	-1.489 [119], -1.489 [103]
	D^{*+}	1.303	1.303 [119], 1.303 [103]
	D_1^0	0.001	0.001 [119]
	D_1^+	0.543	0.543 [119]
	D_2^{*0}	-2.979	-2.979 [119]
	D_2^{*+}	2.141	2.141 [119]

After checking the reliability of the effective masses of the quarks, we proceed to study the M1 radiative decay widths between the isoscalar DN and D^*N molecular pentaquarks. As mentioned earlier, the M1 radiative decay widths between the hadronic molecular states depend on the binding properties for the initial and final hadronic molecular states [102, 103, 110, 111, 115, 116, 119], but the experimental data for the isoscalar DN and D^*N molecular pentaquarks are currently unavailable [121]. Therefore, in the present work we assume the same binding energies for the initial and final

molecular pentaquarks and utilize three representative binding energies of -2 MeV, -8 MeV, and -14 MeV to discuss the M1 radiative decay widths between the isoscalar DN and D^*N molecular pentaquarks.

Based on the above discussions, we can calculate the transition magnetic moments and the M1 radiative decay widths between the isoscalar DN and D^*N molecular pentaquarks by conducting the single channel analysis. The corresponding numerical results are presented in Table II. As shown in Table II, when considering the same binding energies for the initial and final molecular pentaquarks and utilizing three representative binding energies of -2 MeV, -8 MeV, and -14 MeV, the transition magnetic moments of the $D^*N(3/2^-) \rightarrow DN(1/2^-)\gamma$ and $D^*N(1/2^-) \rightarrow DN(1/2^-)\gamma$ processes are approximately $0.634 \sim 0.659 \mu_N$ and $-0.436 \sim -0.431 \mu_N$, respectively. Furthermore, the M1 radiative decay widths of the $D^*N(3/2^-) \rightarrow DN(1/2^-)\gamma$ and $D^*N(1/2^-) \rightarrow DN(1/2^-)\gamma$ processes are about $4.361 \sim 4.711$ keV and $4.025 \sim 4.151$ keV, respectively. For the $D^*N(1/2^-) \rightarrow D^*N(3/2^-)\gamma$ process, the transition magnetic moment is around $-0.468 \sim -0.433 \mu_N$, and the corresponding M1 radiative decay width is zero when taking the same binding energies for the initial and final molecular pentaquarks. This phenomenon is caused by the phase space being zero. When the binding energies of the isoscalar D^*N state with $J^P = 1/2^-$ and the isoscalar D^*N state with $J^P = 3/2^-$ are varied between -2 MeV and -14 MeV, the corresponding M1 radiative decay width for the $D^*N(1/2^-) \rightarrow D^*N(3/2^-)\gamma$ process is less than 0.003 keV, this is mainly due to the small phase space.

Similar to the study of the mass spectrum of the isoscalar DN and D^*N molecular pentaquarks in Ref. [28], we can further consider the contributions of the S - D wave mixing effect and the coupled channel effect to discuss the M1 radiative decay widths between the isoscalar DN and D^*N molecular pentaquarks. Considering the contribution of the S - D wave mixing effect, the relevant spin-orbit wave functions $|^{2S+1}L_J\rangle$ for the isoscalar DN state with $J^P = 1/2^-$, the isoscalar D^*N state with $J^P = 1/2^-$, and the isoscalar D^*N state with $J^P = 3/2^-$ are $|^2S_{1/2}\rangle$, $|^2S_{1/2}\rangle/|^4D_{1/2}\rangle$, and $|^4S_{3/2}\rangle/|^2D_{3/2}\rangle/|^4D_{3/2}\rangle$ [28], respectively. Here, S , L , and J in the spin-orbit wave function are the spin, the orbital angular momentum, and the total angular momentum of the corresponding channel. For the isoscalar DN state with $J^P = 1/2^-$, we can further take into account the influence of the coupled channel effect by including the DN and D^*N channels to discuss the associated electromagnetic properties. When calculating the transition magnetic moment of the D -wave channel, it is necessary to expand the spin-orbital wave function $|^{2S+1}L_J\rangle$ by the coupling of the orbital wave function Y_{Lm_L} and the spin wave function $|S, m_S\rangle$, which can be given by $|^{2S+1}L_J\rangle = \sum_{m_L, m_S} C_{Lm_L, m_S}^{J, M} Y_{Lm_L} |S, m_S\rangle$ [102, 103, 110, 111, 115, 116, 119].

Following the preceding discussions, we can further calculate the transition magnetic moments and the corresponding M1 radiative decay widths between the isoscalar DN and D^*N molecular pentaquarks after considering the contributions of the S - D wave mixing effect and the coupled channel effect. In Table II, we present our obtained transition magnetic moments and M1 radiative decay widths between the isoscalar DN and

TABLE II: The transition magnetic moments and the M1 radiative decay widths between the isoscalar DN and D^*N molecular pentaquarks obtained through the single channel analysis, the S - D wave mixing analysis, and the coupled channel analysis, respectively. Here, we take the same binding energies for the initial and final molecular pentaquarks and consider three representative binding energies of -2 MeV, -8 MeV, and -14 MeV to present the numerical results of the transition magnetic moments and the M1 radiative decay widths between the isoscalar DN and D^*N molecular pentaquarks.

Radiative decays	$\mu_{H \rightarrow H'} (\mu_N)$	$\Gamma_{H \rightarrow H' \gamma} (\text{keV})$
Single channel analysis		
$D^*N(\frac{3}{2}^-) \rightarrow DN(\frac{1}{2}^-)\gamma$	0.634, 0.655, 0.659	4.361, 4.665, 4.711
$D^*N(\frac{1}{2}^-) \rightarrow DN(\frac{1}{2}^-)\gamma$	-0.436, -0.437, -0.431	4.137, 4.151, 4.025
$D^*N(\frac{1}{2}^-) \rightarrow D^*N(\frac{3}{2}^-)\gamma$	-0.468, -0.447, -0.433	0.003 ^a
S - D wave mixing analysis		
$D^*N(\frac{3}{2}^-) \rightarrow DN(\frac{1}{2}^-)\gamma$	0.618, 0.629, 0.626	4.146, 4.300, 4.259
$D^*N(\frac{1}{2}^-) \rightarrow DN(\frac{1}{2}^-)\gamma$	-0.420, -0.413, -0.404	3.837, 3.711, 3.538
$D^*N(\frac{1}{2}^-) \rightarrow D^*N(\frac{3}{2}^-)\gamma$	-0.466, -0.452, -0.445	0.003
Coupled channel analysis		
$D^*N(\frac{3}{2}^-) \rightarrow DN(\frac{1}{2}^-)\gamma$	0.652, 0.687, 0.696	4.677, 5.124, 5.252
$D^*N(\frac{1}{2}^-) \rightarrow DN(\frac{1}{2}^-)\gamma$	-0.411, -0.398, -0.386	3.676, 3.441, 3.230

^aIn this work, the maximum value of the M1 radiative decay width is listed for the decay process involving the same initial and final system, which is obtained by varying the binding energies of the initial and final molecular pentaquarks.

D^*N molecular pentaquarks. These values were determined through the S - D wave mixing analysis and the coupled channel analysis, respectively. By comparing the numerical results obtained from the single channel analysis, we observe that the S - D wave mixing effect and the coupled channel effect do not significantly influence the transition magnetic moments and the M1 radiative decay widths between the isoscalar DN and D^*N molecular pentaquarks, and the change of their M1 radiative decay widths is less than 1 keV.

Since the experimental discoveries of the $\Lambda_c^+(2940)$ and $\Lambda_c^+(2910)$, their inner structures and spin-parity quantum numbers have sparked extensive theoretical discussions [26–47, 49–67]. However, their inner structures and spin-parity quantum numbers have not been conclusively determined until now. In the following, we first discuss whether the corresponding spin-parity quantum numbers of the $\Lambda_c^+(2940)$ and $\Lambda_c^+(2910)$ in the framework of the D^*N molecular states [26–47] can be determined by studying the related M1 radiative decay widths.

- If the $\Lambda_c^+(2940)$ and $\Lambda_c^+(2910)$ can be regarded as the D^*N molecular states with $I(J^P) = 0(3/2^-)$ and $0(1/2^-)$, we find

$$\Gamma_{\Lambda_c^+(2940) \rightarrow DN(1/2^-)\gamma} = 4.675 \sim 5.133 \text{ keV}, \quad (2.13)$$

$$\Gamma_{\Lambda_c^+(2910) \rightarrow DN(1/2^-)\gamma} = 1.501 \sim 1.626 \text{ keV}, \quad (2.14)$$

$$\Gamma_{\Lambda_c^+(2940) \rightarrow \Lambda_c^+(2910)\gamma} = 0.009 \sim 0.011 \text{ keV}, \quad (2.15)$$

$$\frac{\Gamma_{\Lambda_c^+(2940) \rightarrow DN(1/2^-)\gamma}}{\Gamma_{\Lambda_c^+(2910) \rightarrow DN(1/2^-)\gamma}} = 2.875 \sim 3.420. \quad (2.16)$$

- If the $\Lambda_c^+(2940)$ and $\Lambda_c^+(2910)$ can be interpreted as the D^*N molecular states with $I(J^P) = 0(1/2^-)$ and $0(3/2^-)$, we obtain

$$\Gamma_{\Lambda_c^+(2940) \rightarrow DN(1/2^-)\gamma} = 3.455 \sim 4.171 \text{ keV}, \quad (2.17)$$

$$\Gamma_{\Lambda_c^+(2910) \rightarrow DN(1/2^-)\gamma} = 2.047 \sim 2.605 \text{ keV}, \quad (2.18)$$

$$\Gamma_{\Lambda_c^+(2940) \rightarrow \Lambda_c^+(2910)\gamma} = 0.025 \sim 0.026 \text{ keV}, \quad (2.19)$$

$$\frac{\Gamma_{\Lambda_c^+(2940) \rightarrow DN(1/2^-)\gamma}}{\Gamma_{\Lambda_c^+(2910) \rightarrow DN(1/2^-)\gamma}} = 1.326 \sim 2.038. \quad (2.20)$$

For the above mentioned decay processes, we perform the single channel analysis, the S - D wave mixing analysis, and the coupled channel analysis and take the binding energy of the isoscalar DN state with $J^P = 1/2^-$ to be -8 MeV to discuss their M1 radiative decay widths. On the basis of the above discussions, we conclude that the corresponding spin-parity quantum numbers of the $\Lambda_c^+(2940)$ and $\Lambda_c^+(2910)$ in the framework of the D^*N molecular states [26–47] can be determined by studying the related M1 radiative decay widths, especially for the radiative decay ratio $\Gamma_{\Lambda_c^+(2940) \rightarrow DN(1/2^-)\gamma} / \Gamma_{\Lambda_c^+(2910) \rightarrow DN(1/2^-)\gamma}$.

Besides the explanation of the observed $\Lambda_c^+(2940)$ and $\Lambda_c^+(2910)$ as the D^*N molecular states [26–47], they can also be interpreted as the singly charmed baryons $\Lambda_c(2P, 3/2^-)$ and $\Lambda_c(2P, 1/2^-)$ [49–67], respectively. In the following discussions, we explore the possibility of distinguishing different assignments to the $\Lambda_c^+(2940)$ and $\Lambda_c^+(2910)$ by studying the related M1 radiative decay widths. If the $\Lambda_c^+(2940)$ and $\Lambda_c^+(2910)$ can be explained as the D^*N molecular states with $I(J^P) = 0(3/2^-)$ and $0(1/2^-)$ [26–47], we find that the M1 radiative decay width of the $\Lambda_c^+(2940) \rightarrow \Lambda_c^+(2910)\gamma$ process is about 0.01 keV. If the $\Lambda_c^+(2940)$ and $\Lambda_c^+(2910)$ can be assigned as the singly charmed baryons $\Lambda_c(2P, 3/2^-)$ and $\Lambda_c(2P, 1/2^-)$ [49–67], the M1 radiative decay width of the $\Lambda_c^+(2940) \rightarrow \Lambda_c^+(2910)\gamma$ process is around 0.002 keV^2 . Although there exists the obvious difference for the M1 radiative decay width of the $\Lambda_c^+(2940) \rightarrow \Lambda_c^+(2910)\gamma$ process between the hadronic molecular state and the singly charmed baryon interpretations, the corresponding M1 radiative decay width is too small. This presents a significant challenge for the future experimental studies.

C. The M1 radiative decays between the isoscalar D_1N and D_2^*N molecular pentaquarks

In this subsection, we study the M1 radiative decay widths between the isoscalar D_1N and D_2^*N molecular pentaquarks. Similar to the study of the mass spectrum of the isoscalar D_1N and D_2^*N molecular pentaquarks in Ref. [120], we discuss the transition magnetic moments and the M1 radiative decay widths between the isoscalar D_1N and D_2^*N molecular pentaquarks by conducting the S - D wave mixing analysis and the coupled channel analysis. At present, the isoscalar D_1N and D_2^*N molecular pentaquarks are missing experimentally [121]. Thus, in the present work we take the same binding energies for the initial and final molecular pentaquarks and use three representative binding energies of -2 MeV, -8 MeV, and -14 MeV to discuss the transition magnetic moments and the M1 radiative decay widths between the isoscalar D_1N and D_2^*N molecular pentaquarks.

For the isoscalar D_1N and D_2^*N systems, their flavor wave functions can be constructed as [120]

$$|D_1N\rangle = \frac{1}{\sqrt{2}} (|D_1^0p\rangle + |D_1^+n\rangle), \quad (2.21)$$

$$|D_2^*N\rangle = \frac{1}{\sqrt{2}} (|D_2^{*0}p\rangle + |D_2^{*+}n\rangle), \quad (2.22)$$

respectively. When considering the contribution of the S - D wave mixing effect, the relevant spin-orbit wave functions $|^{2S+1}L_J\rangle$ for the isoscalar D_1N state with $J^P = 1/2^+$, the isoscalar D_1N state with $J^P = 3/2^+$, the isoscalar D_2^*N state with $J^P = 3/2^+$, and the isoscalar D_2^*N state with $J^P = 5/2^+$ are $|^2S_{1/2}\rangle/|^4D_{1/2}\rangle$, $|^4S_{3/2}\rangle/|^2D_{3/2}\rangle/|^4D_{3/2}\rangle$, $|^4S_{3/2}\rangle/|^4D_{3/2}\rangle/|^6D_{3/2}\rangle$, and $|^5S_{5/2}\rangle/|^4D_{5/2}\rangle/|^6D_{5/2}\rangle$ [120], respectively. For the isoscalar D_1N state with $J^P = 3/2^+$, we can further consider the influence of the coupled channel effect by including the D_1N and D_2^*N channels to discuss the related electromagnetic properties [120].

With the above preparation, we can study the M1 radiative decay widths between the isoscalar D_1N and D_2^*N molecular pentaquarks by performing the S - D wave mixing analysis and the coupled channel analysis. In Table III, we present our obtained transition magnetic moments and M1 radiative decay widths between the isoscalar D_1N and D_2^*N molecular pentaquarks. These results were obtained through the S - D wave mixing analysis and the coupled channel analysis, respectively.

Based on the results of the transition magnetic moments and the M1 radiative decay widths between the isoscalar D_1N and D_2^*N molecular pentaquarks shown in Table III, we summarize several interesting observations:

1. The study of the M1 radiative decay widths between the isoscalar D_1N and D_2^*N molecular pentaquarks is essential for unravelling their inner structures, which can be used to distinguish the spin-parity quantum numbers of the isoscalar D_1N and D_2^*N molecular pentaquarks in the future experiments. For example, there is a significant difference of the M1 radiative decay widths between the $D_2^*N(5/2^+) \rightarrow D_1N(3/2^+)\gamma$ and

² For the $\Lambda_c^+(2940)$ and $\Lambda_c^+(2910)$, the oscillating parameters $\beta_{\Lambda_c(2P)\rho} = 0.256 \text{ GeV}$ and $\beta_{\Lambda_c(2P)\lambda} = 0.153 \text{ GeV}$ [135] are employed in the simple harmonic oscillator wave function. In addition, we take the diquark mass to be $m_{[ud]} = 0.710 \text{ GeV}$ [85, 104, 114, 136].

TABLE III: The transition magnetic moments and the M1 radiative decay widths between the isoscalar D_1N and D_2^*N molecular pentaquarks obtained through the S - D wave mixing analysis and the coupled channel analysis, respectively. Here, we adopt the same binding energies for the initial and final molecular pentaquarks and use three representative binding energies of -2 MeV, -8 MeV, and -14 MeV to present the numerical results of the transition magnetic moments and the corresponding M1 radiative decay widths between the isoscalar D_1N and D_2^*N molecular pentaquarks.

Radiative decays	$\mu_{H \rightarrow H'} (\mu_N)$	$\Gamma_{H \rightarrow H' \gamma} (\text{keV})$
<i>S</i> - <i>D</i> wave mixing analysis		
$D_1N(\frac{1}{2}^+) \rightarrow D_1N(\frac{3}{2}^+)\gamma$	-0.290, -0.274, -0.266	0.001
$D_2^*N(\frac{5}{2}^+) \rightarrow D_1N(\frac{3}{2}^+)\gamma$	0.366, 0.367, 0.366	0.054, 0.054, 0.054
$D_2^*N(\frac{3}{2}^+) \rightarrow D_1N(\frac{3}{2}^+)\gamma$	-0.190, -0.194, -0.196	0.010, 0.010, 0.010
$D_2^*N(\frac{3}{2}^+) \rightarrow D_1N(\frac{1}{2}^+)\gamma$	0.421, 0.413, 0.408	0.043, 0.041, 0.040
$D_2^*N(\frac{5}{2}^+) \rightarrow D_2^*N(\frac{3}{2}^+)\gamma$	-0.446, -0.408, -0.378	0.004
Coupled channel analysis		
$D_1N(\frac{1}{2}^+) \rightarrow D_1N(\frac{3}{2}^+)\gamma$	-0.267, -0.236, -0.220	0.001
$D_2^*N(\frac{5}{2}^+) \rightarrow D_1N(\frac{3}{2}^+)\gamma$	0.376, 0.384, 0.388	0.057, 0.059, 0.061
$D_2^*N(\frac{3}{2}^+) \rightarrow D_1N(\frac{3}{2}^+)\gamma$	-0.179, -0.173, -0.170	0.009, 0.008, 0.008

$D_2^*N(3/2^+) \rightarrow D_1N(3/2^+)\gamma$ processes. This contrast highlights that the M1 radiative decay widths can offer the theoretical suggestions for the future experimental determination of the spin-parity quantum numbers of the isoscalar D_2^*N molecular pentaquarks.

- By comparing the numerical results obtained from the S - D wave mixing analysis, the coupled channel effect plays a minor role for the M1 radiative decay widths between the isoscalar D_1N and D_2^*N molecular pentaquarks, and the M1 radiative decay widths between the isoscalar D_1N and D_2^*N molecular pentaquarks remain relatively stable when changing the binding energies for the initial and final molecular pentaquarks.
- For the $D_1N(1/2^+) \rightarrow D_1N(3/2^+)\gamma$ and $D_2^*N(3/2^+) \rightarrow D_2^*N(5/2^+)\gamma$ processes, their corresponding M1 radiative decay widths are significantly suppressed. This suppression is attributed to the small phase spaces for both decay processes.
- Compared to the M1 radiative decay widths between the isoscalar DN and D^*N molecular pentaquarks, the M1 radiative decay widths between the isoscalar D_1N and D_2^*N molecular pentaquarks are much smaller. Since the phase space for the $[D^*N] \rightarrow [DN]\gamma$ process is larger than that for the $[D_2^*N] \rightarrow [D_1N]\gamma$ process by around 100 MeV.

III. THE MAGNETIC MOMENT PROPERTIES

In the preceding section, we have discussed the M1 radiative decay characteristics of the isoscalar DN , D^*N , D_1N , and D_2^*N molecular pentaquarks. Our analysis revealed that the M1 radiative decay widths of the isoscalar DN , D^*N , D_1N , and D_2^*N molecular pentaquarks can offer the vital insights into their inner structures. Thus, we strongly encourage our experimental colleagues to focus on the M1 radiative decays of the isoscalar DN , D^*N , D_1N , and D_2^*N molecular pentaquarks.

As another important electromagnetic property unveiling the inner structures of the hadrons, in this section we further study the magnetic moment properties of the isoscalar DN , D^*N , D_1N , and D_2^*N molecular pentaquarks within the constituent quark model. In our specific calculations, we consider the contributions of the S - D wave mixing effect and the coupled channel effect to discuss the magnetic moment properties of the isoscalar DN , D^*N , D_1N , and D_2^*N molecular pentaquarks. Similar to study the M1 radiative decays of the isoscalar DN , D^*N , D_1N , and D_2^*N molecular pentaquarks, we take three representative binding energies of -2 MeV, -8 MeV, and -14 MeV for the isoscalar DN , D^*N , D_1N , and D_2^*N molecular pentaquarks to study their magnetic moment properties when considering the S - D wave mixing effect and the coupled channel effect. In Table IV, we present the magnetic moment properties of the isoscalar DN , D^*N , D_1N , and D_2^*N molecular pentaquarks obtained through the single channel analysis, the S - D wave mixing analysis, and the coupled channel analysis, respectively.

TABLE IV: The magnetic moment properties of the isoscalar DN , D^*N , D_1N , and D_2^*N molecular pentaquarks obtained through the single channel analysis, the S - D wave mixing analysis, and the coupled channel analysis, respectively. The units of the magnetic moments of the hadrons are μ_N . Here, we take three representative binding energies of -2 MeV, -8 MeV, and -14 MeV for the isoscalar DN , D^*N , D_1N , and D_2^*N molecular pentaquarks to present the numerical results of their magnetic moment properties when considering the S - D wave mixing effect and the coupled channel effect. In the first line, Case I, Case II, and Case III correspond to the magnetic moments obtained from the single channel analysis, the S - D wave mixing analysis, and the coupled channel analysis, respectively.

Molecules	Case I	Case II	Case III
$DN(\frac{1}{2}^-)$	0.465	/	0.523, 0.562, 0.579
$D^*N(\frac{3}{2}^-)$	0.372	0.369, 0.367, 0.365	/
$D^*N(\frac{1}{2}^-)$	-0.217	-0.163, -0.115, -0.092	/
$D_1N(\frac{3}{2}^+)$	0.737	0.724, 0.718, 0.715	0.735, 0.735, 0.736
$D_1N(\frac{1}{2}^+)$	0.026	0.040, 0.052, 0.059	/
$D_2^*N(\frac{5}{2}^+)$	0.047	0.043, 0.042, 0.041	/
$D_2^*N(\frac{3}{2}^+)$	-0.656	-0.617, -0.585, -0.569	/

As shown in Table IV, we see that the magnetic moment properties of the isoscalar DN , D^*N , D_1N , and D_2^*N molecu-

lar pentaquarks are the important physical observables unveiling their inner structures. These properties can provide the critical suggestions for determining the spin-parity quantum numbers of the isoscalar DN , D^*N , D_1N , and D_2^*N molecular pentaquarks in the future experimental studies. For example, there exists the significant difference between the isoscalar D^*N state with $J^P = 1/2^-$ and the isoscalar D^*N state with $J^P = 3/2^-$, which depends on their inner structures. By comparing the numerical results obtained from the single channel analysis, we find that the S - D wave mixing effect and the coupled channel effect can affect the magnetic moment properties of the isoscalar DN , D^*N , D_1N , and D_2^*N molecular pentaquarks, but the variation of their magnetic moments is less than $0.13 \mu_N$.

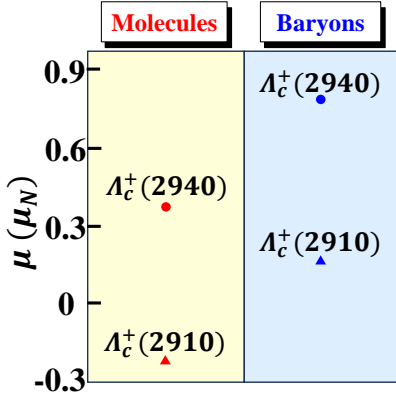


FIG. 1: The magnetic moment properties of the observed $\Lambda_c^+(2940)$ and $\Lambda_c^+(2910)$ within the frameworks of the D^*N molecular states and the $2P$ states of singly charmed baryon, respectively.

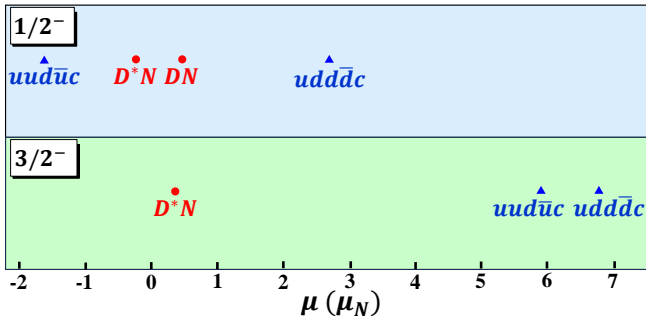


FIG. 2: The comparison focuses on the magnetic moment properties of the single-charm molecular pentaquarks and the single-charm compact pentaquarks [137] with the identical quantum numbers and quark configurations.

From the above analysis, we see that the spin-parity quantum numbers of the isoscalar DN , D^*N , D_1N , and D_2^*N molecular pentaquarks can be distinguished through the study of their magnetic moment properties. In the following, we discuss whether the different theoretical explanations [26–47, 49–67] of the $\Lambda_c^+(2940)$ and $\Lambda_c^+(2910)$ can be clarified by studying their magnetic moment properties. If the $\Lambda_c^+(2940)$ and $\Lambda_c^+(2910)$ can be interpreted as the D^*N molecular states

with $I(J^P) = 0(3/2^-)$ and $0(1/2^-)$ [26–47], we find that the magnetic moments of the $\Lambda_c^+(2940)$ and $\Lambda_c^+(2910)$ are around $0.367 \sim 0.372 \mu_N$ and $-0.051 \sim -0.217 \mu_N$, respectively. If the observed $\Lambda_c^+(2940)$ and $\Lambda_c^+(2910)$ can be explained as the singly charmed baryons $\Lambda_c(2P, 3/2^-)$ and $\Lambda_c(2P, 1/2^-)$ [49–67], then the magnetic moments of the $\Lambda_c^+(2940)$ and $\Lambda_c^+(2910)$ are approximately $0.793 \mu_N$ and $0.156 \mu_N$, respectively. To be more intuitive, we depict the magnetic moment properties of the observed $\Lambda_c^+(2940)$ and $\Lambda_c^+(2910)$ within the frameworks of the D^*N molecular states and the $2P$ states of singly charmed baryon in Fig. 1. As shown in Fig. 1, there is the difference for the magnetic moment properties of the observed $\Lambda_c^+(2940)$ and $\Lambda_c^+(2910)$ within the frameworks of the D^*N molecular states and the $2P$ states of singly charmed baryon. Thus, the different theoretical explanations for the $\Lambda_c^+(2940)$ and $\Lambda_c^+(2910)$ can be clarified by studying the magnetic moment properties in the future experiments.

In Ref. [137], the authors have performed a systematic calculation of the magnetic moment properties of the single-charm compact pentaquarks with $J^P = (1/2^-, 3/2^-, 5/2^-)$. Among them, the $uud\bar{u}c/udd\bar{d}c$ -type single-charm compact pentaquarks and the DN/D^*N -type single-charm molecular pentaquarks may have the same quantum numbers and quark configurations. In Fig. 2, we compare the magnetic moment properties of the single-charm molecular pentaquarks and the single-charm compact pentaquarks with the same quantum numbers and quark configurations. As shown in Fig. 2, we find that there exists the significant differences for the magnetic moment properties of the single-charm molecular pentaquarks and the single-charm compact pentaquarks with the identical quantum numbers and quark configurations. This is particularly evident in the comparison between the D^*N -type single-charm molecular state with $I(J^P) = 0(3/2^-)$ and the $udd\bar{d}c$ -type single-charm compact pentaquark with $I(J^P) = 0(3/2^-)$. Thus, the magnetic moment properties can provide the key observables for distinguishing the single-charm molecular pentaquarks and the single-charm compact pentaquarks with the same quantum numbers and quark configurations.

Based on the above numerical results, the magnetic moment properties of the isoscalar DN , D^*N , D_1N , and D_2^*N molecular pentaquarks are crucial for elucidating their inner structures, which can serve as the crucial clues for distinguishing their spin-parity quantum numbers and configurations in experimental studies. Thus, we look forward the future experiments focusing on the magnetic moment properties of the isoscalar DN , D^*N , D_1N , and D_2^*N molecular pentaquarks.

IV. DISCUSSIONS AND CONCLUSIONS

The hadron spectroscopy is a crucial tool for unravelling the non-perturbative dynamics of the strong interaction. By studying the properties of hadronic states, one can gain valuable insights into the fundamental nature of these interactions, which govern the behavior of quarks and gluons within the confines of hadrons. As an important member of the hadron family, exotic states have attracted considerable attention and

have become a focus of research. A typical example is the observation of the $P_\psi^N(4312)$, $P_\psi^N(4440)$, and $P_\psi^N(4457)$ states [13], which strongly supports the existence of the hidden-charm molecular pentaquark states [16–22]. In the last two decades, the molecular-type multiquarks have been used to decode the properties of these reported new hadronic states [1–11].

Among various molecular-type pentaquarks, the single-charm molecular pentaquarks composed of the charmed mesons and the nucleus have been studied by presenting their partial spectroscopic behavior including the mass spectrum. It is obvious that this is not the whole story of their spectroscopic behavior. In addition, the observed $\Lambda_c^+(2940)$ and $\Lambda_c^+(2910)$ [23–25, 48] can be assigned as the single-charm molecular pentaquark candidates [26–47], but other conventional explanations are available [49–67]. How to distinguish different assignments to the $\Lambda_c^+(2940)$ and $\Lambda_c^+(2910)$ is a challenging task.

Given the current research status, in the present work we systematically study the electromagnetic properties of the single-charm molecular pentaquark candidates, and discuss the electromagnetic properties of the observed $\Lambda_c^+(2940)$ and $\Lambda_c^+(2910)$ in the $2P$ states of singly charmed baryon by adopting the constituent quark model, where both the S - D wave mixing effect and the coupled channel effect are taken into account. In our concrete calculations, we primarily study the M1 radiative decay widths of the isoscalar DN , D^*N , D_1N , and D_2^*N molecular pentaquarks. Our numerical results show that (i) the M1 radiative decay widths between the isoscalar DN , D^*N , D_1N , and D_2^*N molecular pentaquarks provide some insights into their inner structures, which can serve as the crucial clues for distinguishing their spin-parity quantum numbers in the future experimental studies, (ii) the spin-parity quantum numbers of the $\Lambda_c^+(2940)$ and $\Lambda_c^+(2910)$ in the framework of the D^*N molecular states can be clarified by studying their M1 radiative decay widths, especially for the radiative decay ratio $\Gamma_{\Lambda_c^+(2940) \rightarrow DN(1/2^-)\gamma} / \Gamma_{\Lambda_c^+(2910) \rightarrow DN(1/2^-)\gamma}$, and (iii) the M1 radiative decay width of the $\Lambda_c^+(2940) \rightarrow \Lambda_c^+(2910)\gamma$ process can be used to distinguish the theoretical explanations involving the D^*N molecular states and the $2P$ states of singly charmed baryon for the $\Lambda_c^+(2940)$ and $\Lambda_c^+(2910)$.

After that, we study the magnetic moment properties of the

isoscalar DN , D^*N , D_1N , and D_2^*N molecular pentaquarks. From our numerical results, we conclude that the magnetic moment properties of the isoscalar DN , D^*N , D_1N , and D_2^*N molecular pentaquarks can provide the important observables to decipher their inner structures, which can serve as the crucial clues for distinguishing their spin-parity quantum numbers and configurations in experimental studies. In particular, the magnetic moment properties of the observed $\Lambda_c^+(2940)$ and $\Lambda_c^+(2910)$ are different within the frameworks of the D^*N molecular states and the $2P$ states of singly charmed baryon, and the magnetic moment properties of the single-charm molecular pentaquarks and the single-charm compact pentaquarks with the identical quantum numbers and quark configurations exhibit the significant differences.

Since 2015, the significant progress has been made in the study of the hidden-charm molecular pentaquark states. As a potential research topic full of opportunities and challenges, the search for the single-charm molecular pentaquarks will be a new task for the exploration of the pentaquark states in the future experiments. Thus, more theoretical efforts should be made to provide the abundant suggestions for the search of the single-charm molecular pentaquarks. Obviously, the study of the electromagnetic characteristics of the single-charm molecular pentaquark candidates will be an important step in constructing the family of the single-charm molecular pentaquarks.

Acknowledgement

This work is supported by the National Natural Science Foundation of China under Grant Nos. 12335001, 12247155 and 12247101, the China National Funds for Distinguished Young Scientists under Grant No. 11825503, National Key Research and Development Program of China under Contract No. 2020YFA0406400, the 111 Project under Grant No. B20063, the fundamental Research Funds for the Central Universities, and the project for top-notch innovative talents of Gansu province. F.L.W. is also supported by the China Postdoctoral Science Foundation under Grant No. 2022M721440.

-
- [1] X. Liu, An overview of XYZ new particles, *Chin. Sci. Bull.* **59**, 3815 (2014).
 - [2] A. Hosaka, T. Iijima, K. Miyabayashi, Y. Sakai, and S. Yasui, Exotic hadrons with heavy flavors: X , Y , Z , and related states, *Prog. Theor. Exp. Phys.* **2016**, 062C01 (2016).
 - [3] H. X. Chen, W. Chen, X. Liu, and S. L. Zhu, The hidden-charm pentaquark and tetraquark states, *Phys. Rep.* **639**, 1 (2016).
 - [4] J. M. Richard, Exotic hadrons: review and perspectives, *Few Body Syst.* **57**, 1185-1212 (2016).
 - [5] R. F. Lebed, R. E. Mitchell and E. S. Swanson, Heavy-Quark QCD Exotica, *Prog. Part. Nucl. Phys.* **93**, 143-194 (2017).
 - [6] S. L. Olsen, T. Skwarnicki, and D. Zieminska, Nonstandard heavy mesons and baryons: Experimental evidence, *Rev. Mod. Phys.* **90**, 015003 (2018).
 - [7] F. K. Guo, C. Hanhart, U. G. Meißner, Q. Wang, Q. Zhao, and B. S. Zou, Hadronic molecules, *Rev. Mod. Phys.* **90**, 015004 (2018).
 - [8] Y. R. Liu, H. X. Chen, W. Chen, X. Liu, and S. L. Zhu, Pentaquark and tetraquark states, *Prog. Part. Nucl. Phys.* **107**, 237 (2019).
 - [9] N. Brambilla, S. Eidelman, C. Hanhart, A. Nefediev, C. P. Shen, C. E. Thomas, A. Vairo, and C. Z. Yuan, The XYZ states: Experimental and theoretical status and perspectives, *Phys. Rep.* **873**, 1 (2020).
 - [10] L. Meng, B. Wang, G. J. Wang and S. L. Zhu, Chiral perturbation

- tion theory for heavy hadrons and chiral effective field theory for heavy hadronic molecules, *Phys. Rept.* **1019**, 1-149 (2023).
- [11] H. X. Chen, W. Chen, X. Liu, Y. R. Liu and S. L. Zhu, An updated review of the new hadron states, *Rept. Prog. Phys.* **86**, no.2, 026201 (2023).
- [12] R. Aaij *et al.* (LHCb Collaboration), Observation of $J/\psi p$ resonances consistent with pentaquark states in $\Lambda_b^0 \rightarrow J/\psi K^- p$ decays, *Phys. Rev. Lett.* **115**, 072001 (2015).
- [13] R. Aaij *et al.* (LHCb Collaboration), Observation of a narrow pentaquark state, $P_c(4312)^+$, and of two-peak structure of the $P_c(4450)^+$, *Phys. Rev. Lett.* **122**, 222001 (2019).
- [14] R. Aaij *et al.* (LHCb Collaboration), Evidence of a $J/\psi \Lambda$ structure and observation of excited Ξ^- states in the $\Xi_b^- \rightarrow J/\psi \Lambda K^-$ decay, *Sci. Bull.* **66**, 1278-1287 (2021).
- [15] R. Aaij *et al.* (LHCb Collaboration), Observation of a $J/\psi \Lambda$ resonance consistent with a strange pentaquark candidate in $B^- \rightarrow J/\psi \Lambda \bar{p}$ decays, *Phys. Rev. Lett.* **131**, 031901 (2023).
- [16] J. J. Wu, R. Molina, E. Oset and B. S. Zou, Prediction of narrow N^* and Λ^* resonances with hidden charm above 4 GeV, *Phys. Rev. Lett.* **105**, 232001 (2010).
- [17] W. L. Wang, F. Huang, Z. Y. Zhang, and B. S. Zou, $\Sigma_c \bar{D}$ and $\Lambda_c \bar{D}$ states in a chiral quark model, *Phys. Rev. C* **84**, 015203 (2011).
- [18] Z. C. Yang, Z. F. Sun, J. He, X. Liu, and S. L. Zhu, The possible hidden-charm molecular baryons composed of anti-charmed meson and charmed baryon, *Chin. Phys. C* **36**, 6 (2012).
- [19] J. J. Wu, T.-S. H. Lee, and B. S. Zou, Nucleon resonances with hidden charm in coupled-channel Models, *Phys. Rev. C* **85**, 044002 (2012).
- [20] X. Q. Li and X. Liu, A possible global group structure for exotic states, *Eur. Phys. J. C* **74**, 3198 (2014).
- [21] R. Chen, X. Liu, X. Q. Li, and S. L. Zhu, Identifying Exotic Hidden-Charmed Pentaquarks, *Phys. Rev. Lett.* **115**, 132002 (2015).
- [22] M. Karliner and J. L. Rosner, New Exotic Meson and Baryon Resonances from Doubly-Heavy Hadronic Molecules, *Phys. Rev. Lett.* **115**, 122001 (2015).
- [23] B. Aubert *et al.* (BaBar Collaboration), Observation of a charmed baryon decaying to $D^0 p$ at a mass near 2.94 GeV/ c^2 , *Phys. Rev. Lett.* **98** (2007), 012001.
- [24] K. Abe *et al.* (Belle Collaboration), Experimental constraints on the Spin and Parity of the $\Lambda_c^+(2880)$, *Phys. Rev. Lett.* **98** (2007), 262001.
- [25] R. Aaij *et al.* (LHCb Collaboration), Study of the $D^0 p$ amplitude in $\Lambda_b^0 \rightarrow D^0 p \pi^-$ decays, *JHEP* **05** (2017), 030.
- [26] X. G. He, X. Q. Li, X. Liu and X. Q. Zeng, $\Lambda_c^+(2940)$: A Possible molecular state?, *Eur. Phys. J. C* **51** (2007), 883-889.
- [27] C. Garcia-Recio, V. K. Magas, T. Mizutani, J. Nieves, A. Ramos, L. L. Salcedo and L. Tolos, The s -wave charmed baryon resonances from a coupled-channel approach with heavy quark symmetry, *Phys. Rev. D* **79** (2009), 054004.
- [28] J. He, Y. T. Ye, Z. F. Sun and X. Liu, The observed charmed hadron $\Lambda_c(2940)^+$ and the $D^* N$ interaction, *Phys. Rev. D* **82** (2010), 114029.
- [29] Y. Dong, A. Faessler, T. Gutsche and V. E. Lyubovitskij, Strong two-body decays of the $\Lambda_c(2940)^+$ in a hadronic molecule picture, *Phys. Rev. D* **81** (2010), 014006.
- [30] Y. Dong, A. Faessler, T. Gutsche, S. Kumano and V. E. Lyubovitskij, Radiative decay of $\Lambda_c(2940)^+$ in a hadronic molecule picture, *Phys. Rev. D* **82** (2010), 034035.
- [31] W. H. Liang, Y. F. Qiu, J. X. Hu and P. N. Shen, Λ_c^* in a coupled-channel baryon-meson scattering, *Chin. Phys. C* **35** (2011), 16-21.
- [32] Y. Dong, A. Faessler, T. Gutsche, S. Kumano and V. E. Lyubovitskij, Strong three-body decays of $\Lambda_c(2940)^+$, *Phys. Rev. D* **83** (2011), 094005.
- [33] P. G. Ortega, D. R. Entem and F. Fernandez, Quark model description of the $\Lambda_c(2940)^+$ as a molecular $D^* N$ state and the possible existence of the $\Lambda_b(6248)$, *Phys. Lett. B* **718** (2013), 1381-1384.
- [34] J. R. Zhang, S -wave $D^{(*)} N$ molecular states: $\Sigma_c(2800)$ and $\Lambda_c(2940)^{+?}$, *Phys. Rev. D* **89** (2014) no.9, 096006.
- [35] P. G. Ortega, D. R. Entem and F. Fernandez, The $\Lambda_c(2940)^+$ as a $D^* N$ Molecule in a Constituent Quark Model and a Possible $\Lambda_b(6248)$, *Few Body Syst.* **54** (2013) no.7-10, 1101-1104.
- [36] Y. Dong, A. Faessler, T. Gutsche and V. E. Lyubovitskij, Role of the hadron molecule $\Lambda_c(2940)$ in the $p \bar{p} \rightarrow p D^0 \bar{\Lambda}_c(2286)$ annihilation reaction, *Phys. Rev. D* **90** (2014) no.9, 094001.
- [37] P. G. Ortega, D. R. Entem and F. Fernández, Hadronic molecules in the open charm and open bottom baryon spectrum, *Phys. Rev. D* **90** (2014) no.11, 114013.
- [38] J. J. Xie, Y. B. Dong and X. Cao, Role of the $\Lambda_c^+(2940)$ in the $\pi^- p \rightarrow D^- D^0 p$ reaction close to threshold, *Phys. Rev. D* **92** (2015) no.3, 034029.
- [39] D. Yang, J. Liu and D. Zhang, $ND^{(*)}$ and $N\bar{B}^{(*)}$ interactions in a chiral quark model, *arXiv:1508.03883*.
- [40] L. Zhao, H. Huang and J. Ping, ND and $N\bar{B}$ systems in quark delocalization color screening model, *Eur. Phys. J. A* **53** (2017) no.2, 28.
- [41] D. Zhang, D. Yang, X. F. Wang and K. Nakayama, Possible S -wave $ND^{(*)}$ and $N\bar{B}^{(*)}$ bound states in a chiral quark model, *arXiv:1903.01207*.
- [42] B. Wang, L. Meng and S. L. Zhu, $D^{(*)} N$ interaction and the structure of $\Sigma_c(2800)$ and $\Lambda_c(2940)$ in chiral effective field theory, *Phys. Rev. D* **101** (2020) no.9, 094035.
- [43] Y. Yan, X. Hu, Y. Wu, H. Huang, J. Ping and Y. Yang, Pentaquark interpretation of Λ_c states in the quark model, *Eur. Phys. J. C* **83** (2023) no.6, 524.
- [44] Q. Xin, X. S. Yang and Z. G. Wang, The singly charmed pentaquark molecular states via the QCD sum rules, *Int. J. Mod. Phys. A* **38** (2023) no.22n23, 2350123.
- [45] U. Ozdem, Electromagnetic properties of the $\Sigma_c(2800)^+$ and $\Lambda_c(2940)^+$ states via light-cone QCD, *Eur. Phys. J. C* **83** (2023) no.11, 1077.
- [46] M. J. Yan, F. Z. Peng and M. Pavon Valderrama, Molecular charmed baryons and pentaquarks from light-meson exchange saturation, *Phys. Rev. D* **109** (2024) no.1, 014023.
- [47] Z. L. Yue, Q. Y. Guo and D. Y. Chen, Strong decays of the $\Lambda_c(2910)$ and $\Lambda_c(2940)$ in the ND^* molecular frame, *arXiv:2402.10594*.
- [48] Y. B. Li *et al.* (Belle Collaboration), Evidence of a New Excited Charmed Baryon Decaying to $\Sigma_c(2455)^{0,++} \pi^\pm$, *Phys. Rev. Lett.* **130** (2023) no.3, 031901.
- [49] H. Y. Cheng and C. K. Chua, Strong Decays of Charmed Baryons in Heavy Hadron Chiral Perturbation Theory, *Phys. Rev. D* **75** (2007), 014006.
- [50] C. Chen, X. L. Chen, X. Liu, W. Z. Deng and S. L. Zhu, Strong decays of charmed baryons, *Phys. Rev. D* **75** (2007), 094017.
- [51] D. Ebert, R. N. Faustov and V. O. Galkin, Masses of excited heavy baryons in the relativistic quark model, *Phys. Lett. B* **659** (2008), 612-620.
- [52] X. H. Zhong and Q. Zhao, Charmed baryon strong decays in a chiral quark model, *Phys. Rev. D* **77** (2008), 074008.
- [53] X. Liu, Strong decays of newly observed heavy flavor hadrons, *Chin. Phys. C* **33** (2009), 473-480.
- [54] E. Klempt and J. M. Richard, Baryon spectroscopy, *Rev. Mod. Phys.* **82** (2010), 1095-1153.

- [55] B. Chen, D. X. Wang and A. Zhang, J^P Assignments of Λ_c^+ Baryons, *Chin. Phys. C* **33** (2009), 1327-1330.
- [56] H. Y. Cheng, C. Q. Geng and Y. K. Hsiao, Possibly New Charmed Baryon States from $\bar{B}^0 \rightarrow p\bar{p}D^{(*)0}$ Decays, *Phys. Rev. D* **89** (2014) no.3, 034005.
- [57] Q. F. Lü, Y. Dong, X. Liu and T. Matsuki, Puzzle of the Λ_c Spectrum, *Nucl. Phys. Rev.* **35** (2018) no.1, 1-4.
- [58] Q. F. Lü, L. Y. Xiao, Z. Y. Wang and X. H. Zhong, Strong decay of $\Lambda_c(2940)$ as a $2P$ state in the Λ_c family, *Eur. Phys. J. C* **78** (2018) no.7, 599.
- [59] J. J. Guo, P. Yang and A. Zhang, Strong decays of observed Λ_c baryons in the 3P_0 model, *Phys. Rev. D* **100** (2019) no.1, 014001.
- [60] S. Q. Luo, B. Chen, Z. W. Liu and X. Liu, Resolving the low mass puzzle of $\Lambda_c(2940)^+$, *Eur. Phys. J. C* **80** (2020) no.4, 301.
- [61] K. Gandhi, Z. Shah and A. K. Rai, Spectrum of nonstrange singly charmed baryons in the constituent quark model, *Int. J. Theor. Phys.* **59** (2020) no.4, 1129-1156.
- [62] K. Gong, H. Y. Jing and A. Zhang, Possible assignments of highly excited $\Lambda_c(2860)^+$, $\Lambda_c(2880)^+$ and $\Lambda_c(2940)^+$, *Eur. Phys. J. C* **81** (2021) no.5, 467.
- [63] G. L. Yu, Z. Y. Li, Z. G. Wang, J. Lu and M. Yan, Systematic analysis of single heavy baryons Λ_Q , Σ_Q and Ω_Q , *Nucl. Phys. B* **990** (2023), 116183.
- [64] K. Azizi, Y. Sarac and H. Sundu, Interpretation of the $\Lambda_c(2910)^+$ baryon newly seen by Belle Collaboration and its possible bottom partner, *Eur. Phys. J. C* **82** (2022) no.10, 920.
- [65] Z. L. Zhang, Z. W. Liu, S. Q. Luo, F. L. Wang, B. Wang and H. Xu, $\Lambda_c(2910)$ and $\Lambda_c(2940)$ as conventional baryons dressed with the D^*N channel, *Phys. Rev. D* **107** (2023) no.3, 034036.
- [66] G. L. Yu, Y. Meng, Z. Y. Li, Z. G. Wang and L. Jie, Strong decay properties of single heavy baryons Λ_Q , Σ_Q and Ω_Q , *Int. J. Mod. Phys. A* **38** (2023) no.15n16, 2350082.
- [67] H. M. Yang and H. X. Chen, $2P$ -wave charmed baryons from QCD sum rules, *Phys. Rev. D* **109** (2024) no.3, 036032.
- [68] F. Schlumpf, Magnetic moments of the baryon decuplet in a relativistic quark model, *Phys. Rev. D* **48**, 4478-4480 (1993).
- [69] F. Schlumpf, Relativistic constituent quark model of electroweak properties of baryons, *Phys. Rev. D* **47**, 4114 (1993); [*Phys. Rev. D* **49**, 6246 (1994)].
- [70] T. P. Cheng and L. F. Li, Why naive quark model can yield a good account of the baryon magnetic moments, *Phys. Rev. Lett.* **80**, 2789-2792 (1998).
- [71] P. Ha and L. Durand, Baryon magnetic moments in a QCD based quark model with loop corrections, *Phys. Rev. D* **58**, 093008 (1998).
- [72] Y. R. Liu, P. Z. Huang, W. Z. Deng, X. L. Chen and S. L. Zhu, Pentaquark magnetic moments in different models, *Phys. Rev. C* **69**, 035205 (2004).
- [73] P. Z. Huang, Y. R. Liu, W. Z. Deng, X. L. Chen and S. L. Zhu, Heavy pentaquarks, *Phys. Rev. D* **70**, 034003 (2004).
- [74] S. L. Zhu, Pentaquarks, *Int. J. Mod. Phys. A* **19**, 3439-3469 (2004).
- [75] S. Kumar, R. Dhir and R. C. Verma, Magnetic moments of charm baryons using effective mass and screened charge of quarks, *J. Phys. G* **31**, 141-147 (2005).
- [76] A. R. Haghighat, Magnetic Moment of the Pentaquark Θ^+ State, *arXiv:hep-ph/0609253*.
- [77] G. Ramalho, K. Tsushima and F. Gross, A Relativistic quark model for the Omega-electromagnetic form factors, *Phys. Rev. D* **80**, 033004 (2009).
- [78] R. Dhir and R. C. Verma, Magnetic Moments of ($J^P = 3/2^+$) Heavy Baryons Using Effective Mass Scheme, *Eur. Phys. J. A* **42**, 243-249 (2009).
- [79] A. Majethiya, B. Patel and P. C. Vinodkumar, Radiative decays of single heavy flavour baryons, *Eur. Phys. J. A* **42**, 213-218 (2009).
- [80] N. Sharma, H. Dahiya, P. K. Chatley and M. Gupta, Spin $\frac{1}{2}^+$, spin $\frac{3}{2}^+$ and transition magnetic moments of low lying and charmed baryons, *Phys. Rev. D* **81**, 073001 (2010).
- [81] N. Sharma, A. Martinez Torres, K. P. Khemchandani and H. Dahiya, Magnetic moments of the low-lying $1/2^-$ octet baryon resonances, *Eur. Phys. J. A* **49**, 11 (2013).
- [82] R. Dhir, C. S. Kim and R. C. Verma, Magnetic Moments of Bottom Baryons: Effective mass and Screened Charge, *Phys. Rev. D* **88**, 094002 (2013).
- [83] Z. Ghaleenovi, A. A. Rajabi, S. x. Qin and D. H. Rischke, Ground-State Masses and Magnetic Moments of Heavy Baryons, *Mod. Phys. Lett. A* **29**, 1450106 (2014).
- [84] A. Girdhar, H. Dahiya and M. Randhawa, Magnetic moments of $J^P = \frac{3}{2}^+$ decuplet baryons using effective quark masses in chiral constituent quark model, *Phys. Rev. D* **92**, 033012 (2015).
- [85] G. J. Wang, R. Chen, L. Ma, X. Liu and S. L. Zhu, Magnetic moments of the hidden-charm pentaquark states, *Phys. Rev. D* **94**, no.9, 094018 (2016).
- [86] A. Majethiya, K. Thakkar and P. C. Vinodkumar, Spectroscopy and decay properties of Σ_b, Λ_b baryons in quark-diquark model, *Chin. J. Phys.* **54**, 495-502 (2016).
- [87] K. Thakkar, A. Majethiya and P. C. Vinodkumar, Magnetic moments of baryons containing all heavy quarks in the quark-diquark model, *Eur. Phys. J. Plus* **131**, 339 (2016).
- [88] Z. Shah, K. Thakkar, A. K. Rai and P. C. Vinodkumar, Mass spectra and Regge trajectories of Λ_c^+ , Σ_c^0 , Ξ_c^0 and Ω_c^0 baryons, *Chin. Phys. C* **40**, 123102 (2016).
- [89] Z. Shah, K. Thakkar and A. K. Rai, Excited State Mass spectra of doubly heavy baryons Ω_{cc} , Ω_{bb} and Ω_{bc} , *Eur. Phys. J. C* **76**, 530 (2016).
- [90] A. Kaur, P. Gupta and A. Upadhyay, Properties of $J^P = 1/2^+$ baryon octets at low energy, *PTEP* **2017**, 063B02 (2017).
- [91] Z. Shah and A. Kumar Rai, Spectroscopy of the Ω_{ccb} baryon in the hypercentral constituent quark model, *Chin. Phys. C* **42**, 053101 (2018).
- [92] K. Gandhi, Z. Shah and A. K. Rai, Decay properties of singly charmed baryons, *Eur. Phys. J. Plus* **133**, 512 (2018).
- [93] H. Dahiya, Transition magnetic moments of $J^P = \frac{3}{2}^+$ decuplet to $J^P = \frac{1}{2}^+$ octet baryons in the chiral constituent quark model, *Chin. Phys. C* **42**, 093102 (2018).
- [94] V. Simonis, Improved predictions for magnetic moments and M1 decay widths of heavy hadrons, *arXiv:1803.01809*.
- [95] Z. Ghaleenovi and M. Moazzen Sorkhi, Mass spectra and decay properties of Σ_b and Λ_b baryons in a quark model, *Eur. Phys. J. Plus* **133**, 301 (2018).
- [96] K. Gandhi and A. K. Rai, Spectrum of strange singly charmed baryons in the constituent quark model, *Eur. Phys. J. Plus* **135**, 213 (2020).
- [97] S. Rahmani, H. Hassanabadi and H. Sobhani, Mass and decay properties of double heavy baryons with a phenomenological potential model, *Eur. Phys. J. C* **80**, 312 (2020).
- [98] M. W. Li, Z. W. Liu, Z. F. Sun and R. Chen, Magnetic moments and transition magnetic moments of P_c and P_{cs} states, *Phys. Rev. D* **104**, no.5, 054016 (2021).
- [99] A. Hazra, S. Rakshit and R. Dhir, Radiative M1 transitions of heavy baryons: Effective quark mass scheme, *Phys. Rev. D* **104**, 053002 (2021).
- [100] C. Menapara and A. K. Rai, Spectroscopic investigation of

- light strange $S = -1$ Λ , Σ and $S = -2$ Ξ baryons, *Chin. Phys. C* **45**, 063108 (2021).
- [101] C. Deng and S. L. Zhu, T_{cc}^+ and its partners, *Phys. Rev. D* **105**, no.5, 054015 (2022).
- [102] F. L. Wang, H. Y. Zhou, Z. W. Liu and X. Liu, What can we learn from the electromagnetic properties of hidden-charm molecular pentaquarks with single strangeness?, *Phys. Rev. D* **106**, no.5, 054020 (2022).
- [103] H. Y. Zhou, F. L. Wang, Z. W. Liu and X. Liu, Probing the electromagnetic properties of the $\Sigma_c^{(*)}D^{(*)}$ -type doubly charmed molecular pentaquarks, *Phys. Rev. D* **106**, no.3, 034034 (2022).
- [104] F. Gao and H. S. Li, Magnetic moments of hidden-charm strange pentaquark states, *Chin. Phys. C* **46**, no.12, 123111 (2022).
- [105] C. Menapara and A. K. Rai, Spectroscopic Study of Strangeness = -3 Ω^- Baryon, *Chin. Phys. C* **46**, 103102 (2022).
- [106] H. Mutuk, The status of Ξ_{cc}^{++} baryon: investigating quark-diquark model, *Eur. Phys. J. Plus* **137**, 10 (2022).
- [107] A. Kakadiya, Z. Shah and A. K. Rai, Spectroscopy of Ω_{ccc} and Ω_{bbb} baryons, *Int. J. Mod. Phys. A* **37**, no.36, 2250225 (2022).
- [108] C. Menapara and A. K. Rai, Spectroscopy of light baryons: Δ resonances, *Int. J. Mod. Phys. A* **37**, no.27, 2250177 (2022).
- [109] B. Mohan, T. M. S., A. Hazra and R. Dhir, Screening of the quark charge and mixing effects on transition moments and M1 decay widths of baryons, *Phys. Rev. D* **106**, no.11, 113007 (2022).
- [110] F. L. Wang, S. Q. Luo, H. Y. Zhou, Z. W. Liu and X. Liu, Exploring the electromagnetic properties of the $\Xi_c^{(*)}\bar{D}_s^*$ and $\Omega_c^{(*)}\bar{D}_s^*$ molecular states, *Phys. Rev. D* **108**, 034006 (2023).
- [111] F. L. Wang and X. Liu, New type of doubly charmed molecular pentaquarks containing most strange quarks: Mass spectra, radiative decays, and magnetic moments, *Phys. Rev. D* **108**, no.7, 074022 (2023).
- [112] H. T. An, S. Q. Luo, Z. W. Liu and X. Liu, Spectroscopy behavior of fully heavy tetraquarks, *Eur. Phys. J. C* **83**, 740 (2023).
- [113] T. W. Wu and Y. L. Ma, Doubly heavy tetraquark multiplets as heavy antiquark-diquark symmetry partners of heavy baryons, *Phys. Rev. D* **107**, no.7, L071501 (2023).
- [114] F. Guo and H. S. Li, Analysis of the hidden-charm pentaquark states $P_\psi^{N^0}$ based on magnetic moment and transition magnetic moment, *arXiv:2304.10981*.
- [115] F. L. Wang, S. Q. Luo and X. Liu, Radiative decays and magnetic moments of the predicted B_c -like molecules, *Phys. Rev. D* **107**, no.11, 114017 (2023).
- [116] F. L. Wang and X. Liu, Surveying the mass spectra and the electromagnetic properties of the $\Xi_c^{(*)}D^*$ molecular pentaquarks, *Phys. Rev. D* **109**, no.1, 014043 (2024).
- [117] H. S. Li, F. Guo, Y. D. Lei and F. Gao, Magnetic moments and axial charges of the octet hidden-charm molecular pentaquark family, *arXiv:2401.14767*.
- [118] H. S. Li, Ab initio calculation of molecular pentaquark magnetic moments in heavy pentaquark chiral perturbation theory, *arXiv:2401.14759*.
- [119] B. J. Lai, F. L. Wang and X. Liu, Investigating the M1 radiative decay behaviors and the magnetic moments of the predicted triple-charm molecular-type pentaquarks, *arXiv:2402.07195*.
- [120] R. Chen, Z. F. Sun, X. Liu and S. M. Gerasyuta, Predicting exotic molecular states composed of nucleon and P -wave charmed meson, *Phys. Rev. D* **90** (2014) no.3, 034011.
- [121] R. L. Workman *et al.* [Particle Data Group], Review of Particle Physics, *PTEP* **2022**, 083C01 (2022).
- [122] S. Godfrey and R. Kokoski, The Properties of p -Wave Mesons with One Heavy Quark, *Phys. Rev. D* **43**, 1679-1687 (1991).
- [123] T. Matsuki, T. Morii and K. Seo, Mixing angle between 3P_1 and 1P_1 in HQET, *Prog. Theor. Phys.* **124**, 285-292 (2010).
- [124] T. Barnes, N. Black and P. R. Page, Strong decays of strange quarkonia, *Phys. Rev. D* **68**, 054014 (2003).
- [125] Q. T. Song, D. Y. Chen, X. Liu and T. Matsuki, Higher radial and orbital excitations in the charmed meson family, *Phys. Rev. D* **92**, no.7, 074011 (2015).
- [126] B. Aubert *et al.* (BaBar Collaboration), Evidence for $X(3872) \rightarrow \psi(2S)\gamma$ in $B^\pm \rightarrow X(3872)K^\pm$ decays and a study of $B \rightarrow c\bar{c}\gamma K$, *Phys. Rev. Lett.* **102**, 132001 (2009).
- [127] V. Bhardwaj *et al.* (Belle Collaboration), Observation of $X(3872) \rightarrow J/\psi\gamma$ and search for $X(3872) \rightarrow \psi'\gamma$ in B decays, *Phys. Rev. Lett.* **107**, 091803 (2011).
- [128] R. Aaij *et al.* (LHCb Collaboration), Evidence for the decay $X(3872) \rightarrow \psi(2S)\gamma$, *Nucl. Phys. B* **886**, 665 (2014).
- [129] M. Ablikim *et al.* (BESIII Collaboration), Study of open-charm decays and radiative transitions of the $X(3872)$, *Phys. Rev. Lett.* **124**, no.24, 242001 (2020).
- [130] J. Dey, V. Shevchenko, P. Volkovitsky and M. Dey, Radiative decays of S -wave charmed baryons, *Phys. Lett. B* **337**, 185-188 (1994).
- [131] S. Q. Luo, L. S. Geng and X. Liu, Double-charm heptaquark states composed of two charmed mesons and one nucleon, *Phys. Rev. D* **106** (2022) no.1, 014017.
- [132] D. O. Riska and G. E. Brown, Nucleon resonance transition couplings to vector mesons, *Nucl. Phys. A* **679**, 577 (2001).
- [133] S. Godfrey and K. Moats, Properties of Excited Charm and Charm-Strange Mesons, *Phys. Rev. D* **93**, no.3, 034035 (2016).
- [134] V. K. Khersonskii, A. N. Moskalev and D. A. Varshalovich, Quantum Theory Of Angular Momentum, *World Scientific Publishing Company, Singapore*, 1988.
- [135] S. Q. Luo and X. Liu, Investigating the spectroscopy behavior of undetected $1F$ -wave charmed baryons, *Phys. Rev. D* **108**, no.3, 034002 (2023).
- [136] D. Ebert, R. N. Faustov and V. O. Galkin, Masses of tetraquarks with open charm and bottom, *Phys. Lett. B* **696** (2011), 241-245.
- [137] A. Sharma and A. Upadhyay, Masses and Magnetic Moments of Singly Heavy Pentaquarks, *arXiv:2401.02146*.